COBEM 99
XV Congresso Brasileiro de Engenharia Mecânica
15th Brazilian Congress of Mechanical Engineering
22 - 26 de Novembro de 1999 / November 22 - 26, 1999 Águas de Lindóia, São Paulo,

ANALISYS OF LAMINAR FORCED CONVECTION IN ANNULAR DUCTS USING INTEGRAL TRANSFORMS

Luiz M. Pereira
Renato M. Cotta
Laboratório de Transmissão e Tecnologia do Calor, LTTC
Departamento de Engenharia Mecânica, EE/COPPE/UFRJ
Cx. Postal 68503 – Ilha do Fundão – Rio de Janeiro – RJ - Brasil
21945-970, e-mail: mariano@lttc.com.ufrj.br ou cotta@serv.com.ufrj.br
Jesus S. Pérez Guerrero
Coordenação de Rejeitos, COREJ
Comissão Nacional de Energia Nuclear, CNEN
Rua General Severiano, 90 – Botafogo – Rio de Janeiro – RJ – Brasil
22294-900, e-mail: jperez@cnen.gov.br

Abstract. *Laminar forced convection in annular ducts is analyzed by using the Generalized Integral Transform Technique (GITT) to solve the Navier-Stokes and the energy equations in the cylindrical coordinates system. Some cases involving different aspect ratio, given by the relation between internal and external duct diameters, and for Prandtl number Pr≈0.7, are more closely considered in the study. Numerical results are obtained for local temperature profiles, bulk mean temperature and local Nusselt number. Comparisons with previous results in the literature are performed to validate the present simulation.*

Keywords: *Forced Convection, Navier-Stokes Equations, Annular Ducts, Integral Transform*

1. INTRODUCTION

Forced convection inside ducts has received an ever increasing interest of the thermal sciences researchers because of its wide applicability in the process industry and related fields. The precise knowledge of the heat transfer between the duct walls and the fluid is extremely important in the choice of adequate materials and in the optimum design of such equipment. In particular, the flow in the annular region comprehended by circular concentric ducts is of special interest. This flow model occurs in double pipe heat exchangers, in nuclear reactors cooling and various other applications.

Several works have appeared in the literature about the forced convection problem in the entry region of channels. However, in the case of channels of cylindrical geometry, there are only a few involving the full set of Navier-Stokes and energy equations in modeling this physical problem (Fuller & Samuels, 1970). The majority of the existing articles treat this problem using the boundary layer theory, which makes the final results to some extent limited

(Shumway & McEligot, 1971, Coney & El-Shaarawi, 1975). An important results compilation for this class of problems is presented by Shah & Bhatti (1987), for the laminar forced convection situation.

Thus, the present work intends to fill up this gap in the literature, by providing results for the simultaneously developing laminar flow within annular channels, making use of the Generalized Integral Transform Technique (Cotta, 1993). This hybrid approach is particularly suitable for the production of reference results with automatic accuracy control, such as here intended to.

2. PROBLEM FORMULATION

We consider a Newtonian fluid flowing inside the annular space between two concentric circular ducts with dimensionless radius r_1 and r_2 for the internal and external walls, respectively. The inner wall is insulated while the outer wall is kept at a uniform temperature (see Fig. 1). In order to simplify the problem formulation, we consider steady two-dimensional incompressible flow, laminar regimen, constant physical properties and negligible viscous dissipation of heat.

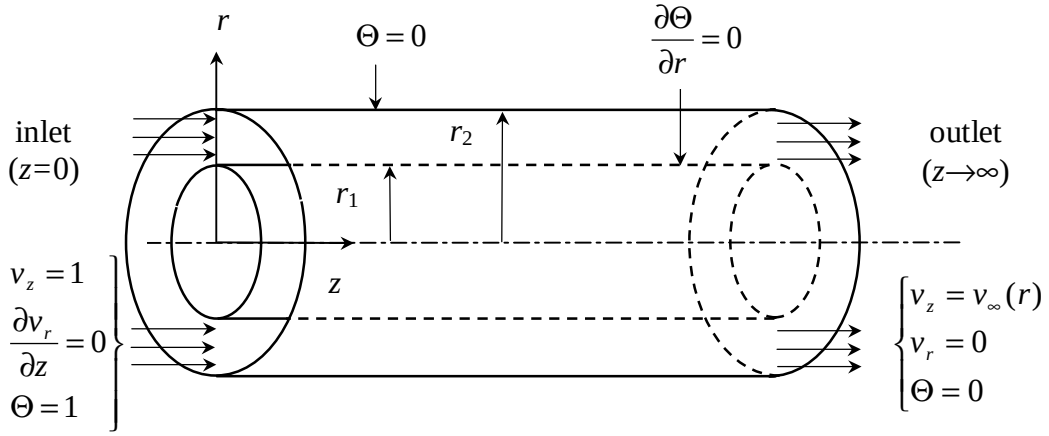

Figure 1 - Geometry, coordinates system and dimensionless boundary conditions of the forced convection problem in annular concentric ducts.

The hydrodynamic study of this problem was developed by Pereira et al. (1998) and we here intend to focus our attention on the thermal part of the problem. According to that previous work, the streamfunction-only formulation for the Navier-Stokes equations is preferable to the primitive variables choice, due to some advantages in its computational solution and further for automatically satisfying the continuity equation and eliminating the pressure gradient from the momentum equations. These conclusions can also be observed in previous works (Pérez Guerrero & Cotta, 1995, 1996) dealing with the Navier-Stokes equations solved by integral transform techniques.

Therefore, the dimensionless energy equation, under the boundary conditions shown in Fig. 1, is written as:

$$\nabla^2\Theta(z,r) = \frac{\mathrm{Pe}}{2(1-\kappa)}\left[\frac{1}{r}\frac{\partial\psi(z,r)}{\partial z}\frac{\partial\Theta(z,r)}{\partial r} - \frac{1}{r}\frac{\partial\psi(z,r)}{\partial r}\frac{\partial\Theta(z,r)}{\partial z}\right] \tag{1}$$

where ∇^2 is the Laplacian operator, and the axial and radial velocity components are defined in terms of the streamfunction, respectively, by:

$$v_z(z,r) = -\frac{1}{r}\frac{\partial \psi(z,r)}{\partial r} \quad \text{and} \quad v_r(z,r) = \frac{1}{r}\frac{\partial \psi(z,r)}{\partial z} \tag{2.a,b}$$

The following dimensionless groups were utilized:

$$v_r = \frac{V_R}{\overline{V}_o}; \quad v_z = \frac{V_Z}{\overline{V}_o}; \quad \Theta = \frac{T - T_w}{T_o - T_w}; \quad r = \frac{R}{R_2}; \quad z = \frac{Z}{R_2}; \quad \mathrm{Re} = \frac{\rho \overline{V}_o D_h}{\mu} \tag{3.a-f}$$

$$\mathrm{Pr} = \frac{\mu c_p}{k}; \quad \mathrm{Pe} = \mathrm{Re}.\mathrm{Pr}; \quad \kappa = \frac{R_1}{R_2}; \quad D_h = 2(R_2 - R_1) \tag{3.g-j}$$

where $v_r(z,r)$ and $v_z(z,r)$ are the dimensionless velocity components in the radial and axial directions, respectively, r and z are the dimensionless radial and axial coordinates, Re is the Reynolds number, $\Theta(z,r)$ is the dimensionless temperature, Pr is the Prandtl number, Pe is the Peclet number, κ is the aspect ratio and D_h is the hydraulic diameter. The parameters ρ, μ, c_p and k are density, absolute viscosity, specific heat at constant pressure and thermal conductivity, respectively. $\overline{V}_o$ is the uniform velocity at the entry section of the duct.

3. SOLUTION

Due to the presence of the hydrodynamic terms in the energy equation, we apply in these terms the same filter used by Pereira et al. (1998), based on the fully developed flow region, to make the boundary conditions of the momentum equations homogeneous in the radial direction. Then, Eq. (1) becomes:

$$\nabla^2 \Theta(z,r) = \frac{\mathrm{Pe}}{2(1-\kappa)}\left[\frac{1}{r}\frac{\partial \varphi(z,r)}{\partial z}\frac{\partial \Theta(z,r)}{\partial r} - \frac{1}{r}\frac{\partial \Theta(z,r)}{\partial z}\left(\frac{\partial \varphi(z,r)}{\partial r} + \frac{d\psi_\infty(r)}{dr}\right)\right] \tag{4}$$

where the streamfunction was divided in two parts, as:

$$\psi(r,z) = \varphi(r,z) + \psi_\infty(r) \tag{5}$$

3.1. Auxiliary Problem

Following the GITT formalism, the thermal eigenvalue problem is easily chosen from the diffusion operator in a hollow cylinder, as:

$$\frac{d^2\Gamma_m(r)}{dr^2} + \frac{1}{r}\frac{d\Gamma_m(r)}{dr} + \xi_m^2 \Gamma_m(r) = 0, \text{ for } \kappa < r < 1 \text{ and } m=1,2,3,... \tag{6.a}$$

where $\Gamma_m(r)$ and ξ_m are the eigenfunctions and eigenvalues, respectively. The boundary conditions are similar to those of the original problem (Eq. 4), i.e.,

$$\frac{d\Gamma_m(\kappa)}{dr} = 0, \quad \text{and} \quad \Gamma_m(1) = 0 \tag{6.b,c}$$

The solution of this eigenvalue problem is given by Ozisik (1993). Therefore,

$$\Gamma_m(r) = \mathrm{J}_o(\xi_m r)\mathrm{Y}_o(\xi_m) - \mathrm{J}_o(\xi_m)\mathrm{Y}_o(\xi_m r) \tag{7}$$

and the transcendental equation to obtain the corresponding eigenvalues is given by:

$$\mathrm{J}'_o(\xi_m \kappa)\mathrm{Y}_o(\xi_m) - \mathrm{J}_o(\xi_m)\mathrm{Y}'_o(\xi_m \kappa) = 0 \tag{8}$$

The eigenfunctions given by Eq. (7) obey the following orthogonality property:

$$\int_{\kappa}^{1} r\,\Gamma_{\mathrm{m}}(r)\Gamma_{\mathrm{n}}(r)\,dr = \begin{cases} 0, & m \neq n \\ M_m, & m = n \end{cases} \tag{9}$$

where M_m is the norm, defined by:

$$M_m = \frac{2}{\pi^2}\frac{\mathrm{J}'^2_o(\xi_m \kappa) - \mathrm{J}^2_o(\xi_m)}{\xi_m^2 \mathrm{J}'^2_o(\xi_m \kappa)}\ , \tag{10}$$

J_o represents the Bessel function of first kind and zero order and Y_o represents the modified Bessel function of first kind and zero order.

3.2. Integral Transform Pair

The integral transform pair for the thermal problem is obtained from the orthogonality property (Eq. 9), and results in:

$$\overline{\Theta}_m(z) = \int_{\kappa}^{1} r\,\widetilde{\Gamma}_m(r)\,\Theta(r,z)\,dr \quad \text{(Transform)} \tag{11.a}$$

$$\Theta(r,z) = \sum_{m=1}^{\infty} \widetilde{\Gamma}_m(r)\,\overline{\Theta}_m(z) \qquad \text{(Inverse)} \tag{11.b}$$

where, $\widetilde{\Gamma}_m(r) = \dfrac{\Gamma_m(r)}{M_m^{\,1/2}}$ (12)

is the normalized eigenfunction for the temperature field.

3.3. Integral Transform Solution

Applying the operator $\int_{\kappa}^{1} r\,\widetilde{\Gamma}_m(r)\,dr$ in the partial differential equation (Eq. 4), making use of the inverse formulae (Eq.11.b) and considering the orthogonality property (Eq. 9), we obtain a infinite system of ordinary differential equations, as a function of the *z* position only, which is given by:

$$\overline{\Theta}_m''(z) = \xi_m^2 \overline{\Theta}_m(z) + \frac{\mathrm{Pe}}{2(1-\kappa)} \left\{ \sum_{n=1}^{\infty} \left[C_{mn\infty} \overline{\Theta}_n'(z) + \sum_{j=1}^{\infty} \left(A_{mnj} \overline{\Theta}_n(z) \overline{\varphi}_j'(z) - B_{mnj} \overline{\Theta}_n'(z) \overline{\varphi}_j(z) \right) \right] \right\} \tag{13.a}$$

The same procedure is adopted to transform the boundary conditions in *z* direction, which results in:

$$\overline{\Theta}_m(0) = \int_{\kappa}^{1} r \, \widetilde{\Gamma}_m(r) \, dr \qquad \text{and} \qquad \overline{\Theta}_m(\infty) = 0 \tag{13.b.c}$$

The integral coefficients appearing in Eq. (13.a) result from the non-transformable terms and are defined by:

$$A_{mnj} = \int_{\kappa}^{1} \widetilde{\Gamma}_m(r) \, \widetilde{\Gamma}_n'(r) \, \widetilde{\Omega}_j(r) \, dr \tag{14.a}$$

$$B_{mnj} = \int_{\kappa}^{1} \widetilde{\Gamma}_m(r) \, \widetilde{\Gamma}_n(r) \, \widetilde{\Omega}_j'(r) \, dr \tag{14.b}$$

$$C_{mn\infty} = \int_{\kappa}^{1} r \, \widetilde{\Gamma}_m(r) \, \widetilde{\Gamma}_n(r) \, v_{\infty}(r) \, dr \tag{14.c}$$

where $\widetilde{\Omega}_j$ is the eigenfunction of the hydrodynamic auxiliary problem and $v_{\infty}(r)$ is the fully developed velocity profile, both given by Pereira et al. (1998).

These coefficients are obtained numerically using a subroutine available in the IMSL package (IMSL Library, 1987), which implements a reliable error control scheme.

3.4. Ordinary Differential System Solution

The boundary condition at the channel outlet is specified as an open flow boundary condition, and the semi-infinite longitudinal domain [0,∞] is transformed into a finite domain [0,1] to avoid the uncertainty of identifying the adequate position of the fully developed region. The analytical transformation proposed was:

$$\zeta = 1 - \frac{1}{1 + \varepsilon z} \tag{15}$$

where ζ is the transformed axial coordinate and ε is a scale contraction factor, which makes it possible to amplify the transformed channel entry region as much as convenient for computational purposes.

For the solution of the ordinary differential system it is necessary to truncate the infinite system to a sufficiently large finite order NT. The truncated system is solved numerically through well-established computational procedures available in scientific subroutine packages such as the IMSL subroutine BVPFD (IMSL Library, 1987), which implements an adaptively refined grid and a controlled global error scheme. Results are here reported for a requested relative error within 10^{-4} for the transformed potentials.

To conclude the computational procedure, the truncation order NT is automatically established by the inclusion in the computational code of the global error control expression given below, based in the analytical expression for the temperature field:

$$Tol_{\Theta} = \max_{(z,r)} \left| \frac{\sum_{m=NT+1}^{NT+\Delta NT} \tilde{\Gamma}_m(r)\overline{\Theta}_m(z)}{\sum_{m=1}^{NT+\Delta NT} \tilde{\Gamma}_m(r)\overline{\Theta}_m(z)} \right| \tag{16}$$

and NT is increased in fixed steps until convergence is achieved within user specified global accuracy at requested locations.

After the transformed potentials are obtained, we recover the original temperature fields making use of the inversion formulae (Eq. 11.b). The bulk mean temperature (Θ_b) and the local Nusselt number for the outer wall (Nu_2) are calculated through the following equations:

$$\Theta_b(z) = \frac{\int_{\kappa}^{1} \Theta(z,r)\, v_z(z,r)\, r\, dr}{\int_{\kappa}^{1} v_z(z,r)\, r\, dr}; \quad Nu_2 = -\frac{2(1-\kappa)\left.\frac{\partial \Theta(z,r)}{\partial r}\right|_{r=1}}{\Theta_b(z)} \tag{17.a, b}$$

4. RESULTS AND DISCUSSION

Results for aspect ratios κ=0.25, 0.5 and 0.9 and Reynolds number Re=2000 are listed below, considering Prandtl number for air (Pr≈0.7). An equal truncation order for the hydrodynamic and thermal eigenseries (NV=NT) was utilized. Firstly, an analysis of convergence for the bulk mean temperature and local Nusselt number is made and illustrated in tabular form for various truncation orders and different positions along the duct.

With the goal of validating the computational code, initially we calculate the bulk mean temperature and the local Nusselt number for positions corresponding to the definition of the dimensionless axial coordinate utilized in boundary layer approach, which makes this coordinate independent of Reynolds and Prandtl numbers:

$$z^{+} = \frac{z}{2(1-\kappa).\mathrm{Re}.\mathrm{Pr}} \tag{18}$$

Table 1 shows the convergence behavior of the bulk mean temperature difference ($1-\Theta_b$), for aspect ratio κ=0.25 and Re=2000. It can be seen that even a low order of truncation (e.g. NT=21) is enough to furnish a reasonable solution to most engineering needs. The convergence for the local Nusselt number at the outer wall is illustrated in Table 2 for the same parameters defined above. We notice a slower convergence when compared to the bulk mean temperature. This behavior occurs due to the presence of the temperature gradient in its definition, which produces an eigenvalue in the numerator of the Nusselt number expression.

Similarly to the hydrodynamic part, the region away from the entry shows a faster convergence than those positions closer to the inlet of the channel.

The results presented in Tables 1 and 2 were compared with those obtained by Shumway & McEligot (1971) through the boundary layer approach. Here it is observed that these results show a good agreement for intermediate positions and for the region away from the channel

entry. However, in regions close to the channel inlet, the results present a marked discrepancy. This behavior was expectable since the boundary layer formulation is in general more accurate in regions not so close to the channel inlet.

Table 1. Convergence behavior for bulk mean temperature difference $(1-\Theta_b)$ with κ=0.25, Re=2000 and Pr=0.72.

z^+	NT=21	25	27	29	Ref.✚
1.00E-4	2.319E-2	2.344E-2	2.352E-2	2.356E-2	2.310E-2
2.50E-4	3.752E-2	3.742E-2	3.738E-2	3.735E-2	3.660E-2
5.00E-4	5.321E-2	5.304E-2	5.297E-2	5.290E-2	5.205E-2
1.00E-3	7.561E-2	7.536E-2	7.526E-2	7.517E-2	7.430E-2
2.50E-3	1.209E-1	1.206E-1	1.204E-1	1.203E-1	1.195E-1
5.00E-3	1.731E-1	1.728E-1	1.727E-1	1.726E-1	1.718E-1
1.00E-2	2.490E-1	2.487E-1	2.486E-1	2.485E-1	2.477E-1
2.50E-2	4.045E-1	4.043E-1	4.042E-1	4.041E-1	4.038E-1
5.00E-2	5.791E-1	5.789E-1	5.789E-1	5.788E-1	5.785E-1
1.00E-1	7.864E-1	7.863E-1	7.863E-1	7.862E-1	7.857E-1
2.50E-1	9.720E-1	9.720E-1	9.720E-1	9.720E-1	9.715E-1

✚ Shumway & McEligot (1971) – Boundary layer formulation

Table 2. Convergence behavior for local Nusselt number at outer tube wall (Nu_2) with κ=0.25, Re=2000 and Pr=0.72.

z^+	NT=21	25	27	29	Ref.✚
1.00E-4	4.374E+1	4.180E+1	4.070E+1	3.975E+1	3.773E+1
2.50E-4	2.478E+1	2.451E+1	2.447E+1	2.441E+1	2.451E+1
5.00E-4	1.782E+1	1.772E+1	1.767E+1	1.764E+1	1.784E+1
1.00E-3	1.302E+1	1.298E+1	1.297E+1	1.295E+1	1.308E+1
2.50E-3	8.865E+0	8.856E+0	8.854E+0	8.852E+0	8.893E+0
5.00E-3	6.826E+0	6.824E+0	6.823E+0	6.823E+0	6.838E+0
1.00E-2	5.460E+0	5.460E+0	5.460E+0	5.460E+0	5.474E+0
2.50E-2	4.494E+0	4.495E+0	4.495E+0	4.495E+0	4.496E+0
5.00E-2	4.261E+0	4.261E+0	4.261E+0	4.261E+0	4.259E+0
1.00E-1	4.233E+0	4.233E+0	4.233E+0	4.233E+0	4.231E+0
2.50E-1	4.232E+0	4.232E+0	4.232E+0	4.232E+0	4.231E+0

✚ Shumway & McEligot (1971) – Boundary layer formulation

Figure 2 presents the dimensionless temperature convergence behavior for κ=0.5, Re=2000 and Pr=0.7 in a position located next to the channel entry (z=0.35). We notice that for very low orders of truncation, the behavior is quite oscillatory. When NT is increased this oscillation is rapidly damped until graphic convergence is attained for NT>13. In Fig. 3 is illustrated the temperature field development along the duct, obtained with NT=30 in the truncated series solution. One can observed the severe temperature gradients next to the outer tube wall for the positions close to the inlet region of the channel, while these gradients are progressively reduced when increasing the distance from the entry, until the fully developed regime is reached.

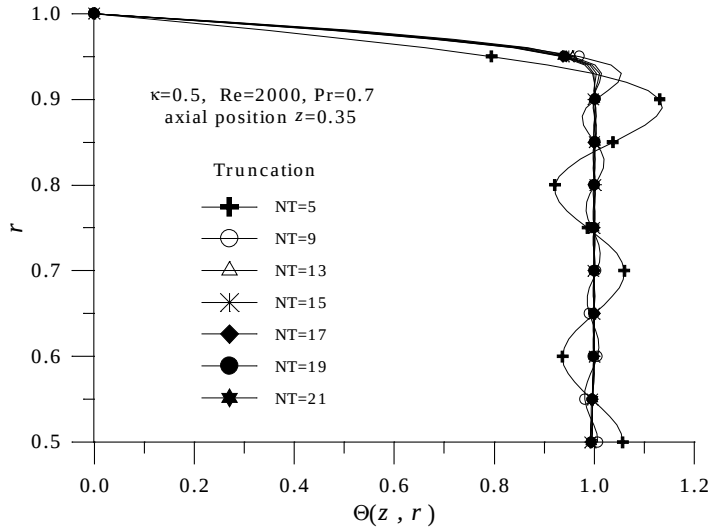

Figure 2 - Temperature convergence behavior for z=0.35, κ=0.5, Re=2000 and Pr=0.7.

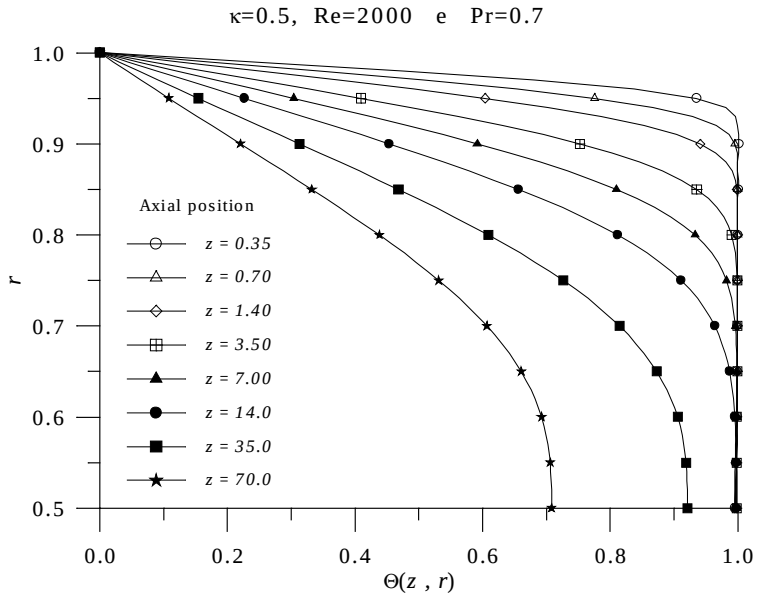

Figure 3 - Temperature profiles along the channel with κ =0.5, Re=2000 and Pr=0.7.

In order to calculate the local Nusselt number and the bulk mean temperature at the same positions given by Coney & El-Shaarawi (1975), we make use of yet another definition of the axial coordinate, as:

$$z^{++} = \frac{2z(1-\kappa)}{\mathrm{Re}} \tag{19}$$

Figure 4 describes the local Nusselt number variation along the outer duct wall for aspect ratios κ=0.5 and 0.9, Re=2000 and Pr=0.7. It is then evident that the local Nusselt number increases when the aspect ratio decreases. Also, it is observed a marked discrepancy between the present results and the boundary layer formulation results, for positions close to the channel entry.

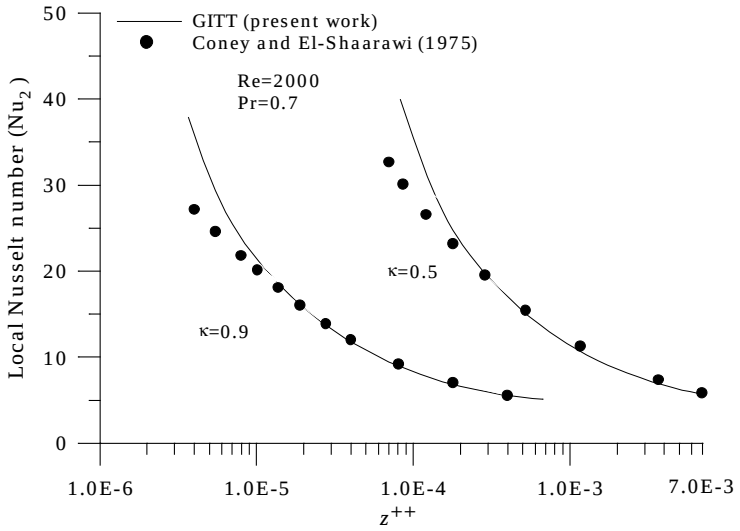

Figure 4 - Local Nusselt number distribution along the axial position with Re=2000 and Pr=0.7, for κ=0.5 and 0.9.

Figures 5 and 6 illustrate the behavior of the bulk mean temperature difference profiles $(1-\Theta_b)$ along the axial direction, for aspect ratios κ=0.5 and 0.9, respectively, and for Re=2000. We observe that increasing aspect ratio, the thickness of the thermal boundary layer decreases. Then, the results obtained by the boundary layer approach for larger aspect ratios present a better agreement with this work, as can also be observed in Fig. 6. Both Figs. 5 and 6, show a tendency to a linear bulk mean temperature variation for positions far from the channel entry, as the flow proceeds towards the fully developed region.

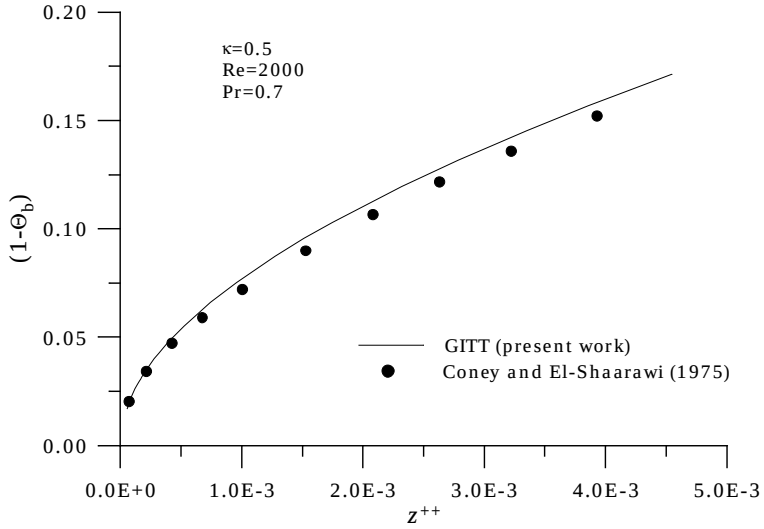

Figure 5 - Bulk mean temperature along the axial position with κ=0.5, Re=2000 and Pr=0.7.

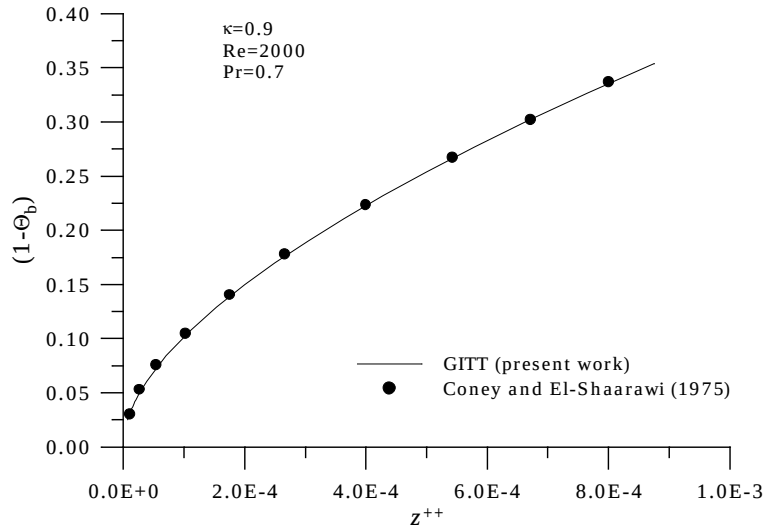

Figure 6 - Bulk mean temperature along the axial position with κ=0.9, Re=2000 and Pr=0.7.

5. CONCLUSIONS

The full set of Navier-Stokes and energy equations is employed to model simultaneously developing flow inside annular ducts. The Generalized Integral Transform Technique is utilized for the error-controlled solution of the proposed mathematical model.

The excellent convergence behavior of the eigenfunction expansions is illustrated, in both tabular and graphical forms. Numerical results for quantities of practical interest are obtained and critically compared against previous results produced through the boundary layer formulation, demonstrating the limitations inherent to this approximation.

REFERENCES

Coney, J. E. R. & El-Shaarawi, M. A. I., 1975, Finite Difference Analysis for Laminar Flow Heat Transfer in Concentric Annuli with Simultaneously Developing Hydrodynamic and Thermal Boundary Layers, Int. J. Num. Meth. Eng., v. 9, pp. 17-38.

Cotta, R. M., 1993, Integral Transforms in Computational Heat and Fluid Flow. Boca Raton, FL, CRC Press.

Fuller, R. E. & Samuels, M. R., 1970, Simultaneous Development of the Velocity and Temperature Fields in the Entry Region of an Annulus, Chem. Eng. Prog. Symp. Series, v. 67, n. 113, pp. 71-77.

IMSL Library, 1987, Math/Lib., Houston, Texas.

Ozisik, M. N., 1993, Heat Conduction. 2nd ed., New York, John Wiley & Sons.

Pereira, L. M., Perez Guerrero, J. S. & Cotta, R. M., 1998, Integral Transformation of the Navier-Stokes Equations in Cylindrical Geometry, Comp. Mech., v. 21, n. 1, pp. 60-70.

Perez Guerrero, J. S. & Cotta, R. M., 1995, Integral Transform Solution of Developing Laminar Duct Flow in Navier-Stokes Formulation, Int. J. Num. Meth. Fluids, v. 20, pp. 1203-1213.

Perez Guerrero, J. S. & Cotta, R. M., 1996, Benchmark Integral Transform Results for Flow Over a Backward-Facing Step, Computers & Fluids, v. 25, n. 5, pp. 527-540.

Shah, R. K. & Bhatti, M. S., 1987, Laminar Convective Heat Transfer in Ducts, In: Kakaç, S., Shah, R. K. and Aung, W. (eds.), Handbook of Single-Phase Convective Heat Transfer, Chapter 3, New York, USA, John Wiley & Sons.

Shumway, R. W. & McEligot, D. M., 1971, Heated Laminar Gas Flow in Annuli with Temperature-Dependent Transport Properties, Nucl. Sci. & Eng., v. 46, pp. 394-407.